Fusion and quasifission dynamics in the reactions ^{48}Ca+^{249}Bk and ^{50}Ti+^{249}Bk using a time-dependent Hartree-Fock approach

A. S. Umar, V. E. Oberacker, and C. Simenel

Fusion and quasifission dynamics in the reactions ^{48}Ca+^{249}Bk and ^{50}Ti+^{249}Bk using a time-dependent Hartree-Fock approach

A. S. Umar,[1, *] V. E. Oberacker,[1, †] and C. Simenel[2, ‡]

[1]*Department of Physics and Astronomy, Vanderbilt University, Nashville, Tennessee 37235, USA*
[2]*Department of Nuclear Physics, Research School of Physics and Engineering,*
The Australian National University, Canberra ACT 2601, Australia

Background: Synthesis of superheavy elements (SHE) with fusion-evaporation reactions is strongly hindered by the quasifission (QF) mechanism which prevents the formation of an equilibrated compound nucleus and which depends on the structure of the reactants. New SHE have been recently produced with doubly-magic ^{48}Ca beams. However, SHE synthesis experiments with single-magic ^{50}Ti beams have so far been unsuccessful.

Purpose: In connection with experimental searches for $Z = 117, 119$ superheavy elements, we perform a theoretical study of fusion and quasifission mechanisms in ^{48}Ca,^{50}Ti+^{249}Bk reactions in order to investigate possible differences in reaction mechanisms induced by these two projectiles.

Methods: The collision dynamics and the outcome of the reactions are studied using unrestricted time-dependent Hartree-Fock (TDHF) calculations as well as the density-constrained TDHF method to extract the nucleus-nucleus potentials and the excitation energy in each fragment.

Results: Nucleus-nucleus potentials, nuclear contact times, masses and charges of the fragments, as well as their kinetic and excitation energies strongly depend on the orientation of the prolate ^{249}Bk nucleus. Long contact times associated with fusion are observed in collisions of both projectiles with the side of the ^{249}Bk nucleus, but not on collisions with its tip. The energy and impact parameter dependencies of the fragment properties, as well as their mass-angle and mass-total kinetic energy correlations are investigated.

Conclusions: Entrance channel reaction dynamics are similar with both ^{48}Ca and ^{50}Ti projectiles. Both are expected to lead to the formation of a compound nucleus by fusion if they have enough energy to get in contact with the side of the ^{249}Bk target.

I. INTRODUCTION

The synthesis of superheavy elements is one of the most fascinating and challenging tasks in low-energy heavy-ion physics. Nuclear mean-field theories predict a superheavy island of stability as a result of new proton and neutron shell closures. Most recent theoretical calculations yield a magic neutron number $N = 184$, but there is no consensus yet about the corresponding magic proton number, with predictions [1–6] ranging from $Z = 114 - 126$. Experimentally, two approaches have been used for the synthesis of these elements. The first method uses targets containing doubly-magic spherical nuclei such as ^{208}Pb (or alternatively ^{209}Bi). By bombarding these targets with heavy-ion beams ranging from chromium to zinc, researchers at the GSI Helmholtz Center in Germany and at Riken were able to produce several isotopes of elements $Z = 107 - 112$. The beam energy was kept low to minimize the excitation energy (cold fusion) [7–11]. The second approach, pioneered at JINR in Russia, uses actinide targets instead. In contrast to the spherical ^{208}Pb target nuclei used at GSI, all of the actinide target nuclei exhibit quadrupole deformed ground states. Target materials ranging from ^{238}U to ^{249}Cf were irradiated with a ^{48}Ca beam. Despite the fact that the excitation energy is found to be substantially higher

in these experiments ('hot-fusion') researchers at JINR were able to create isotopes of elements $Z = 113 - 118$ [12–16], with lifetimes of milliseconds up to a minute. Recently, hot-fusion experiments were also carried out at GSI, LBNL, and RIKEN [10, 17–22] which confirmed the discovery of elements $Z = 112 - 117$.

However, attempts to synthesize even heavier elements such as $Z = 119, 120$ with beams of ^{50}Ti and ^{54}Cr instead of ^{48}Ca have so far not been successful. The experimental community is asking for theoretical guidance as to why ^{48}Ca beams seem to be so crucial in forming superheavy elements. For example, the reaction ^{48}Ca+^{249}Bk produces superheavy element 117 with cross-sections of $2 - 3$ picobarns. By contrast, an upper cross section limit of only 50 fb was reported for the production of isotopes of element 119 in the reaction ^{50}Ti+^{249}Bk at GSI-TASCA [23].

Experimentally it is found that capture reactions involving actinide target nuclei result either in fusion or in quasifission. Fusion produces a compound nucleus in statistical equilibrium, while quasifission leads to a reseparation of the fragments after partial mass equilibration without formation of an equilibrated compound nucleus [24]. Furthermore, if the nucleus does not quasifission and evolves to a compound system, it can still undergo statistical fission due to its excitation. The evaporation residue cross-section is dramatically reduced due to the quasifission (QF) and fusion-fission (FF) processes.

Quasifission occurs at a much shorter time-scale than fusion-fission [25–27]. Consequently, quasifission is the primary reaction mechanism that limits the formation of superheavy nuclei [28–30]. This motivated intensive experi-

---

* umar@compsci.cas.vanderbilt.edu
† volker.e.oberacker@vanderbilt.edu
‡ cedric.simenel@anu.edu.au

mental studies [25–27, 31–48]. These studies have shown a strong impact of the entrance channel characteristics, including deformation [32, 33, 35–37] and shell structure [42] of the reactants. The later stages of the dynamics are also impacted by the fissility of the total system [40, 43], its neutron richness [46], and by shell effects in the exit channel [25, 26, 34, 37, 38, 45, 49–51].

Most dynamical models [52–56] argue that for heavy systems a dinuclear complex is formed initially and the barrier structure and the excitation energy of this precompound system will determine its survival to breaking up via quasifission. The challenge for nuclear theory is to describe the entrance channel dynamics leading either to fusion or to quasifission, as well as the dynamical evolution of the dinuclear complex toward a compound nucleus. Theoretically, this is often done within macroscopic or microscopic-macroscopic approaches [57–62]. As a fully microscopic approach, TDHF is also able to describe the evolution of two colliding nuclei toward a merged system. It can then be used to study the competition between fusion and quasifission up to a time scale of a few 10^{-20}s. For a given initial condition, a TDHF calculation gives a probability of 0 or 1 for quasifission to have occurred at this time. Another way of stating this is that TDHF is a deterministic theory, where for a given initial condition there is only one possible outcome. For longer times the absence of residual interaction in TDHF prevents the formation of a truly equilibrated compound nucleus. Thus, TDHF is ideally suited to study what is sometimes referred to as "fast" quasifission. By the same token, since TDHF theory does not include beyond mean-field correlations only the most probable outcome is observed, while experimentally a distribution is measured. This is most evident in comparison of mass-angle distributions (MAD) with experimental observations [42, 45, 46], where the TDHF results reproduce the properties which can be extracted from expectation values of one-body observable [63], namely the average properties of these distributions. For a more direct comparison with experiment, theories that go beyond the mean-field approximation are necessary. In particular, realistic predictions of mass and charge distributions would require the inclusion of beyond mean-field fluctuations, e.g., within the time-dependent random phase approximation (TDRPA) [64, 65] or with stochastic mean-field approaches [66]. Such beyond mean-field approaches, however, are at least an order of magnitude more expansive in terms of computational time and are beyond the scope of this work.

In this paper we will concentrate on the theoretical analysis of the ^{48}Ca $+^{249}$Bk experiments [13, 14, 22] in which element $Z = 117$ was produced. This system will be compared to the ^{50}Ti $+^{249}$Bk reaction which appears to have a very low cross section limit for synthesizing element $Z = 119$. Our goal is to investigate potential different mechanisms between these two reactions by calculating dynamical observables such as nuclear contact times, mass and charge transfer, excitation energies, and heavy-ion potentials.

A brief introduction to the theoretical framework is provided in section II, followed by a presentation and discussion of the results in section III. Conclusions are drawn in section IV.

II. FORMALISM: TDHF AND DC-TDHF

The Time-Dependent Hartree-Fock (TDHF) theory allows us to study a large variety of phenomena observed in low energy nuclear physics [67, 68]. In particular, TDHF provides a dynamic quantum many-body description of large amplitude collective motion including collective surface vibrations and giant resonances [69–82], nuclear reactions in the vicinity of the Coulomb barrier, such as fusion [83–96], deep-inelastic reactions and transfer [65, 97–103], and dynamics of (quasi)fission fragments [45, 104–111]. The classification of various reaction types in TDHF is done by calculating the time evolution of expectation values of one-body observables: fragments centers of masses, mass and charges on each side of the neck, kinetic energy, orbital angular momentum, among others. Quasifission is characterized by two final state fragments that emerge after a long lived composite system (typically longer than 5 zs) and final fragment masses $A_f = A_{CN}/2 \pm 20$ or more. In addition final TKE's distinguish quasifission from highly damped deep-inelastic collisions, which have a smaller mass and charge difference between initial and final fragments. In TDHF the mass and charge difference between the initial nuclei and the final fragments measure the number of nucleons transferred. As discussed above fusion corresponds to the case where the final product remains as a single composite.

The TDHF equations for the single-particle wave functions

$$h(\{\phi_\mu\}) \, \phi_\lambda(r,t) = i\hbar \frac{\partial}{\partial t} \phi_\lambda(r,t) \quad (\lambda = 1,...,A) , \quad (1)$$

can be derived from a variational principle. The main approximation in TDHF is that the many-body wave function $\Phi(t)$ is assumed to be a single time-dependent Slater determinant at all times. It describes the time-evolution of the single-particle wave functions in a mean-field corresponding to the dominant reaction channel. During the past decade it has become numerically feasible to perform TDHF calculations on a 3D Cartesian grid without any symmetry restrictions and with much more accurate numerical methods [68, 71, 100, 112–116]. Furthermore, the quality of effective interactions has been substantially improved [117–120].

Recently, we have developed a new dynamic microscopic approach, the density-constrained time-dependent Hartree-Fock (DC-TDHF) method [121], to calculate nucleus-nucleus potentials $V(R)$, mass parameters $M(R)$, and precompound excitation energies $E^*(R)$ [122], directly from microscopic TDHF dynamics. The basic idea of this approach is the following: At certain times t or, equivalently, at certain internuclear distances $R(t)$ the instantaneous TDHF density is used to perform a static energy minimization while constraining the proton and neutron densities to be equal to the instantaneous TDHF densities. This can be accomplished by solving the density-constrained density-functional problem

$$E_{DC}(t) = \min_{\rho_n, \rho_p} \left\{ E[\rho_n, \rho_p] + \int d\mathbf{r}\, v_n(\mathbf{r}) \left[\rho_n(\mathbf{r}) - \rho_n^{TDHF}(\mathbf{r}, t)\right] + \int d\mathbf{r}\, v_p(\mathbf{r}) \left[\rho_p(\mathbf{r}) - \rho_p^{TDHF}(\mathbf{r}, t)\right] \right\} , \qquad (2)$$

where $E[\rho_n, \rho_p]$ is the TDHF density-functional (calculated with Skyrme interactions). The quantities $v_{n,p}(\mathbf{r})$ are Lagrange multipliers which represent external fields that constrain the densities during the minimization procedure. This means we allow the single-particle wave functions to rearrange themselves in such a way that the total energy is minimized, subject to the TDHF density constraint. In a typical DC-TDHF run, we utilize a few thousand time steps, and the density constraint is applied every $10 - 20$ time steps. We refer to the minimized energy as the "density constrained energy" $E_{DC}(R(t))$. The ion-ion interaction potential $V(R)$ is obtained by subtracting the constant binding energies E_{A_1} and E_{A_2} of the two individual nuclei

$$V(R) = E_{DC}(R) - E_{A_1} - E_{A_2} . \qquad (3)$$

The calculated ion-ion interaction barriers contain all of the dynamical changes in the nuclear density during the TDHF time-evolution in a self-consistent manner.

In addition to the ion-ion potential it is also possible to obtain coordinate dependent mass parameters. One can compute the "effective mass" $M(R)$ [123] using the conservation of energy in a central collision

$$M(R) = \frac{2[E_{\text{c.m.}} - V(R)]}{\dot{R}^2} , \qquad (4)$$

where the collective velocity $\dot{R}$ is directly obtained from the TDHF time evolution and the potential $V(R)$ from the density constraint calculations. At large distance R, the mass $M(R)$ is equal to the reduced mass μ of the system. At smaller distances, when the nuclei overlap, the mass parameter generally increases. This microscopic approach also applies to reactions involving deformed nuclei when calculations are done in an unrestricted three-dimensional box where the nuclei can be given arbitrary orientations with respect to the collision axis [124–126].

Using the density constrained energy defined above, we can compute the excitation energy of the system at internuclear distance $R(t)$ as follows

$$E^*(R(t)) = E_{TDHF} - E_{DC}(R(t)) - E_{kin}(R(t)) . \qquad (5)$$

where E_{TDHF} is the conserved TDHF energy. The last term denotes the collective kinetic energy

$$E_{kin} \approx \frac{m}{2} \sum_q \int d^3r\, \mathbf{j}_q(\mathbf{r}, t)^2 / \rho_q(\mathbf{r}, t) , \qquad (6)$$

where $\mathbf{j}(\mathbf{r}, t)$ is the local current density from TDHF and m the nucleon mass. The index q denotes the isospin index for neutrons and protons ($q = n, p$).

III. NUMERICAL RESULTS

A. Unrestricted TDHF calculations: fusion and quasifission

In this paper, we focus on fusion and quasifission in the reactions $^{48}\text{Ca} + ^{249}\text{Bk}$ and $^{50}\text{Ti} + ^{249}\text{Bk}$. In our TDHF calculations we use the Skyrme SLy4 and SLy4d energy density functionals [117, 127] including all of the relevant time-odd terms in the mean-field Hamiltonian. Both interactions are constructed using the same fitting procedure, apart for one-body center of mass corrections, included in SLy4, which are small in heavy systems such as those studied here. The $^{48}\text{Ca} + ^{249}\text{Bk}$ calculations were done with SLy4d while the calculations for $^{50}\text{Ti} + ^{249}\text{Bk}$ used the SLy4 parametrization. The reason for switching to SLy4 was due to the availability of the pairing force parameters for this force. To describe these reactions with a high degree of accuracy, the shapes of the individual nuclei must be correctly reproduced by the mean-field theory. In some cases, it is necessary to include BCS pairing which increases the number of single-particle levels that must be taken into account by about 50 percent. Static Hartree-Fock (HF) calculations without pairing predict a spherical density distribution for ^{48}Ca while ^{249}Bk shows prolate quadrupole and hexadecupole deformation, in agreement with experimental data. However, static HF calculations without pairing predict a prolate quadrupole deformation for ^{50}Ti due to partial filling of $\pi f_{7/2}$ with occupation numbers 0 or 1, thus breaking spherical symmetry. When BCS pairing is added, these occupation number are lower than 1 and distributed around the Fermi surface, restoring a spherical density in ^{50}Ti. Therefore, we include BCS pairing (using fixed partial occupations) in the TDHF runs for $^{50}\text{Ti} + ^{249}\text{Bk}$ while pairing has been left out for the system $^{48}\text{Ca} + ^{249}\text{Bk}$ to speed up the calculations.
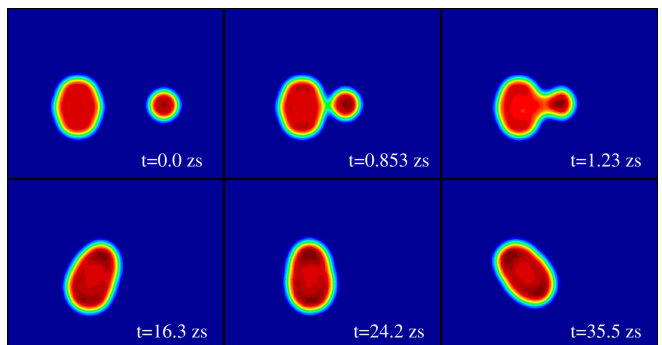

FIG. 1. (Color online) Fusion in the reaction $^{50}\text{Ti} + ^{249}\text{Bk}$ at $E_{\text{c.m.}} = 233$ MeV with impact parameter $b = 0.5$ fm. Shown is a contour plot of the time evolution of the mass density. Time increases from left to right and top to bottom.

Numerically, we proceed as follows: First we generate very well-converged static HF wave functions for the two nuclei on

the 3D grid. The initial separation of the two nuclei is 30 fm with nuclei in their ground states. The nuclei are assumed to arrive to this separation on a Coulomb trajectory for the purpose of initializing the proper boosts. Independent calculation of E2+E4 Coulomb excitation of the ground state rotational bands in a similar system showed that the excitation is small due to the small charge of ^{48}Ca [87]. We have also started at larger distances but did not not notice any appreciable difference in the outcome to warrant the extra computing time. This is because the QF dynamics and outcome is essentially determined by the evolution of the system after contact. In the second step, we apply a boost operator to the single-particle wave functions. The time-propagation is carried out using a Taylor series expansion (up to orders $10 - 12$) of the unitary mean-field propagator, with a time step $\Delta t = 0.4$ fm/c. For reactions leading to superheavy dinuclear systems, the TDHF calculations require very long CPU times: a single TDHF run at fixed $E_{c.m.}$ energy and fixed impact parameter b takes about 1-2 weeks of CPU time on a 16-processor LINUX workstation. A total CPU time of about 6 months was required for all of the calculations presented in this paper.
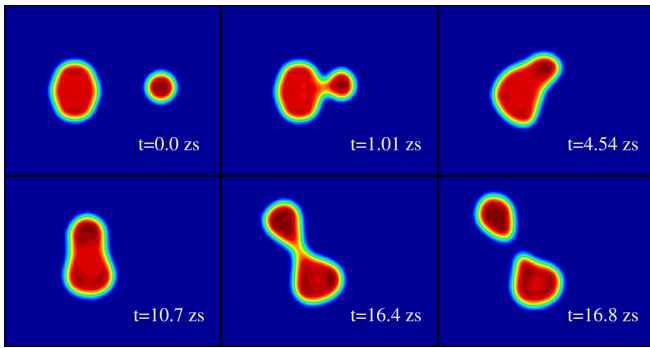

FIG. 2. (Color online) Quasifission in the reaction ^{50}Ti $+^{249}$ Bk at $E_{c.m.} = 233$ MeV with impact parameter $b = 1.0$ fm. Shown is a contour plot of the time evolution of the mass density. Time increases from left to right and top to bottom.

Let us first consider the reaction ^{50}Ti $+^{249}$ Bk at $E_{c.m.} = 233$ MeV, which is the energy used in the GSI-TASCA experiment [23]. The numerical calculations were carried out on a 3D Cartesian grid which spans $(66 \times 52 \times 30)$ fm. In Fig. 1 we show contour plots of the mass density in the $x - z$ plane as a function of time. In this case, the initial orientation of the ^{249}Bk nucleus has been chosen such that the ^{50}Ti projectile collides with the "side" of the deformed target nucleus. We observe that at an impact parameter $b = 0.5$ fm TDHF theory predicts fusion. Our conceptual definition of fusion is an event with large contact time exceeding $25 - 35$ zs, and in addition we require a mononuclear shape without any neck formation.

By contrast, at an impact parameter $b = 1.0$ fm TDHF theory predicts quasifission, see Fig. 2. As the nuclei approach each other, a neck forms between the two fragments which grows in size as the system begins to rotate. Due to the Coulomb repulsion and centrifugal forces, the dinuclear system elongates and forms a very long neck which eventually ruptures leading to two separated fragments. In this case, the

contact time is found to be 16 zs.
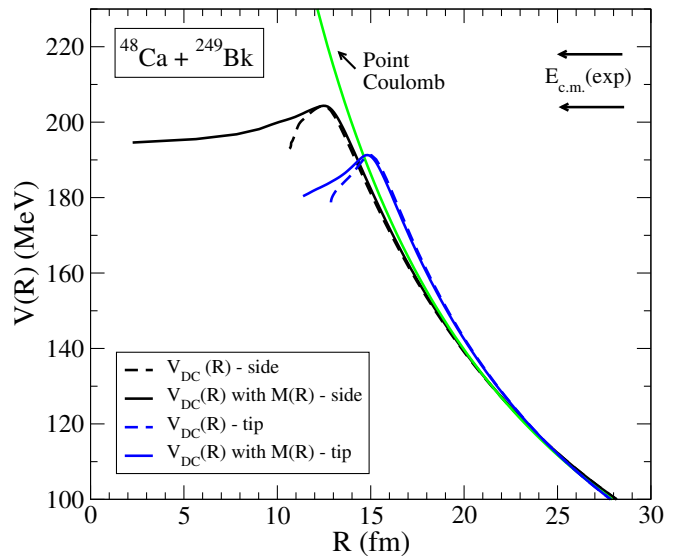
B.   Nucleus-nucleus potentials (DC-TDHF)

FIG. 3.   (Color online) Nucleus-nucleus potential, $V(R)$, for the ^{48}Ca $+^{249}$ Bk system obtained from DC-TDHF calculation for selected orientation angles of the ^{249}Bk nucleus. Also shown is the range of the experimental c.m. energies.

In Fig. 3 we plot the microscopic DC-TDHF nucleus-nucleus potential barriers for the ^{48}Ca $+^{249}$ Bk system. The dashed lines correspond to potentials calculated with constant reduced mass, while the solid lines include the influence of the coordinate-dependent "effective mass" $M(R)$. We observe that the coordinate-dependent mass changes only the interior region of the potential barriers. The barriers are depicted for two extreme orientations of the ^{249}Bk nucleus (tip and side). As expected, the tip orientation of ^{249}Bk results in a significantly lower barrier, E_B(tip)$= 191.22$ MeV located at internuclear distance R_B(tip)$= 15.04$ fm, as compared to the side orientation, E_B(side)$= 204.36$ MeV with R_B(side)$= 12.47$ fm. (For comparison, in the phenomenological Bass model for two spherical nuclei one obtains a barrier height E_B(Bass)$= 203.1$ MeV located at an internuclear distance R_B(Bass)$= 12.8$ fm.) Also shown is the range of experimental energies at which this reaction has been studied, $E_{c.m.} = 204 - 218$ MeV in the Dubna experiment [14] and $E_{c.m.} = 211 - 218$ MeV in the GSI-TASCA experiment [22]. We conclude that the highest experimental energy $E_{c.m.} = 218$ MeV is above both barriers but the lowest experimental energy $E_{c.m.} = 204$ MeV is slightly below the barrier for the side orientation of ^{249}Bk.

In Fig. 4 we plot the corresponding potential barriers for the ^{50}Ti $+^{249}$ Bk system. Again, the tip orientation of ^{249}Bk results in a significantly lower barrier, E_B(tip)$= 211.2$ MeV located at internuclear distance R_B(tip)$= 14.48$ fm, as compared to the side orientation, E_B(side)$= 224.6$ MeV with R_B(side)$= 12.96$ fm. (For comparison, in the phenolog-
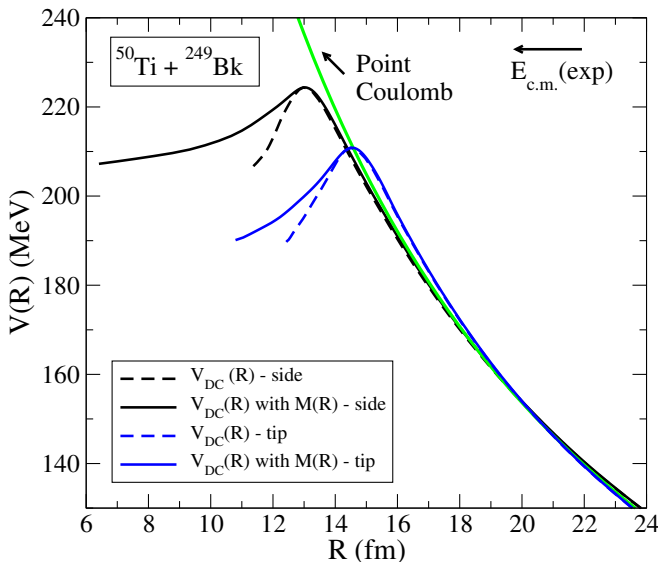
FIG. 4. (Color online) Nucleus-nucleus potential, $V(R)$, for the ^{50}Ti $+^{249}$Bk system obtained from DC-TDHF calculation for selected orientation angles of the ^{249}Bk nucleus. Also shown is the energy $E_{c.m.} = 233.2$ MeV used in the GSI-TASCA experiment.

FIG. 5. (Color online) (a) Contact time, (b) mass and charge of the light fragment, and (c) excitation energy E^* of the heavy and light fragments as a function of $E_{c.m.}$ for central collisions of ^{48}Ca with ^{249}Bk. Solid lines are for the side orientation of the deformed ^{249}Bk nucleus, and dashed lines are for the tip orientations.

ical Bass model for two spherical nuclei one obtains a barrier height E_B(Bass)= 223.7 MeV located at an internuclear distance R_B(Bass)= 12.8 fm.) Also shown is the experimental energy (at the center of target) $E_{c.m.} = 233.2$ MeV used in the GSI-TASCA experiment [22]. We note that the chosen experimental energy is 22.0 MeV above the barrier E_B(tip) and 8.6 MeV above the barrier E_B(side).

C. Energy dependence for central collision

We define the contact time as the time interval between the time t_1 when the two nuclear surfaces (defined as isodensities with half the saturation density $\rho_0/2 = 0.08$ fm^{-3}) first merge into a single surface and the time t_2 when the surface splits up again. Figure 5 (a) shows the contact time as a function of center-of-mass energy for central collisions of ^{48}Ca with ^{249}Bk calculated in TDHF. For the tip orientation of the ^{249}Bk nucleus (dashed line) we observe contact times of order $10 - 12$ zs which are essentially constant over a wide range of energies, $E_{c.m.} = 193 - 230$ MeV. Only at energies below the potential barrier, E_B(tip)= 192.2 MeV, do the contact times drop off very rapidly because these events correspond to inelastic scattering and few-nucleon transfer reactions. A dramatically different picture emerges for the side orientation of the ^{249}Bk nucleus (solid line): At energies above the barrier E_B(side)= 205.4 MeV, the contact times rise very steeply with energy and reach values up to 22 zs at $E_{c.m.} = 210$ MeV. For energies above this value, TDHF predicts fusion. In our TDHF calculations, we have found fusion events at energies $E_{c.m.} = 211, 212, 218, 220$ MeV for the side orientation.

Figure 5 (b) shows the corresponding mass and charge of the light fragment. We observe that the mass and charge
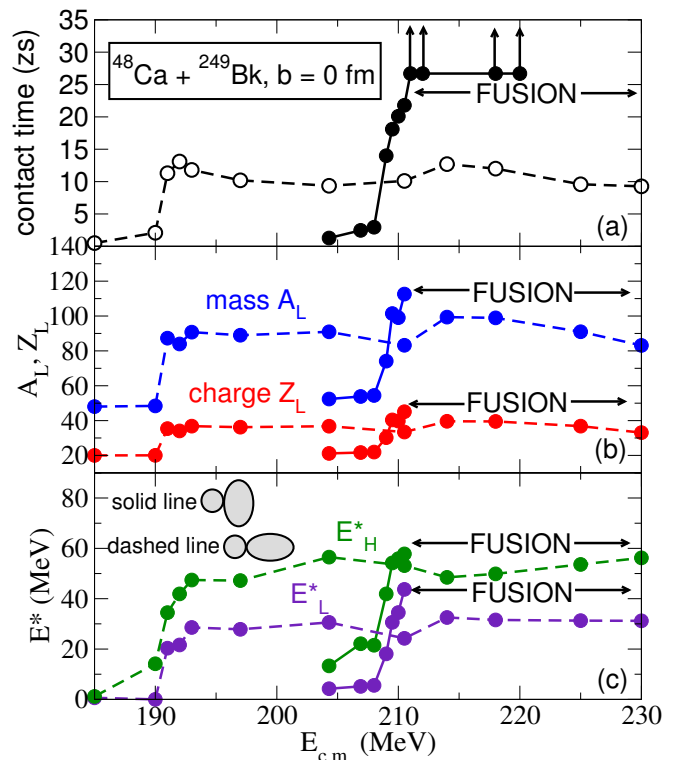
transfer to the light fragment are roughly proportional to the nuclear contact time. In particular, for the side orientation of ^{249}Bk, we find quasielastic collisions at energies below $E_{c.m.} = 204$ MeV. Quasifission is limited to the narrow energy window $E_{c.m.} = 209 - 211$ MeV, whereas for energies above 211 MeV we find fusion. Naturally, non-central impact parameters can show quasifission in the range where we see fusion. The quasifission results are very different for the tip orientation of ^{249}Bk, ranging over a much wider energy domain from $E_{c.m.} = 193$ MeV to the highest energy of 230 MeV studied here, with a lower maximum mass and charge transfer compared to the side orientation of ^{249}Bk. Tip collisions clearly favor production of a heavy fragment near ^{208}Pb (with a ^{91}Rb light fragment) due to magic shell effects at all energies. A similar phenomenon was already observed in TDHF calculations of reactions with ^{238}U [45, 111]. In some cases, a light fragment with $N = 50$ is formed, indicating an influence of this magic number in the dynamics as well.

Recently, we have developed an extension to TDHF theory via the use of a density constraint to calculate the excitation energy of *each fragment* directly from the TDHF density evolution. This gives us new information on the repartition of the excitation energy between the heavy and light fragments which is not directly available in standard TDHF calculations unless one uses advanced projection techniques [102]. In Fig. 5 (c) we show the excitation energies of the two frag-

ments at internuclear distances of $26-30$ fm. In collisions with the tip of the ^{249}Bk nucleus, we find quasifission excitation energies of $E_H^* = 34-56$ MeV for the heavy fragment and $E_L^* = 20-32$ MeV for the light fragment, respectively. For the side orientation, quasifission is only found in the narrow energy window $E_{c.m.} = 209-211$ MeV, with corresponding excitation energies of $E_H^* = 42-58$ MeV and $E_L^* = 18-44$ MeV.

Figure 6 shows the corresponding results for central collisions of ^{50}Ti with ^{249}Bk. The contact times and the masses
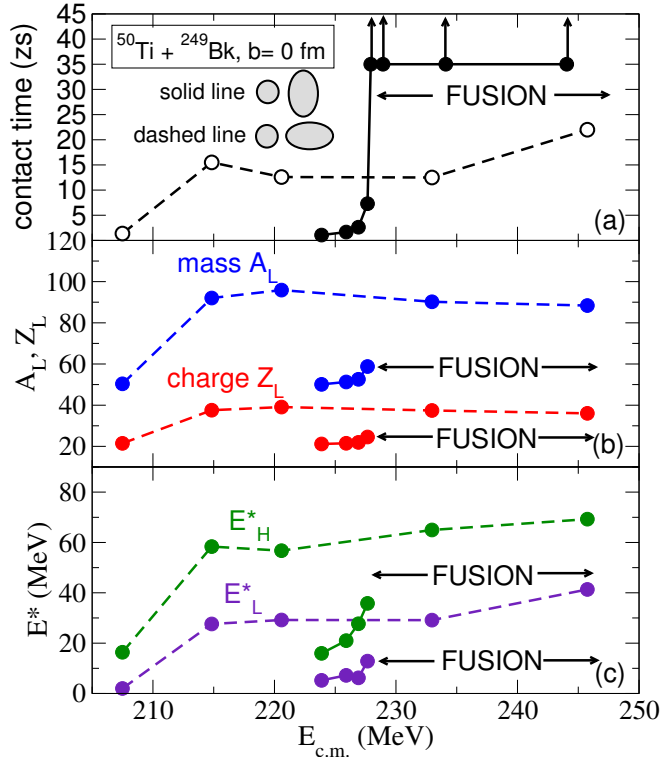

FIG. 6. (Color online) (a) Contact time, (b) mass and charge of the light fragment, and (c) excitation energy E^* of the heavy and light fragments as a function of $E_{c.m.}$ for central collisions of ^{50}Ti with ^{249}Bk. Solid lines are for the side orientation of the deformed ^{249}Bk nucleus, and dashed lines are for the tip orientations.

and charges of the light fragment show a similar behavior as a function of the center-of-mass energy as compared to the ^{48}Ca $+^{249}$Bk reaction. For the tip orientation, we find quasifission for $E_{c.m.} \geq 214$ MeV, with excitation energies of $E_H^* = 57-69$ MeV for the heavy fragment and $E_L^* = 27-41$ MeV for the light fragment, respectively. The mass and charge of the fragments indicate a strong influence of the shell effects in the ^{208}Pb region, as in reactions with ^{48}Ca. However, $N = 50$ does not seem to play a role here. For the side orientation, we find inelastic and multi-nucleon transfer reactions at energies $E_{c.m.} = 223-227$ MeV. Quasifission is confined to an extremely narrow energy window around $E_{c.m.} = 227.4-227.7$ MeV, with excitation energies of $E_H^* \simeq 36$ MeV and $E_L^* \simeq 13$ MeV. At energies $E_{c.m.} > 228$ MeV, fusion sets in.

D. Impact parameter dependence at fixed energy

For the ^{48}Ca $+^{249}$Bk system, we now examine the impact parameter dependence of the same observables at a fixed energy of $E_{c.m.} = 218$ MeV which is the highest energy used in both the Dubna and GSI-TASCA experiments. Let us first
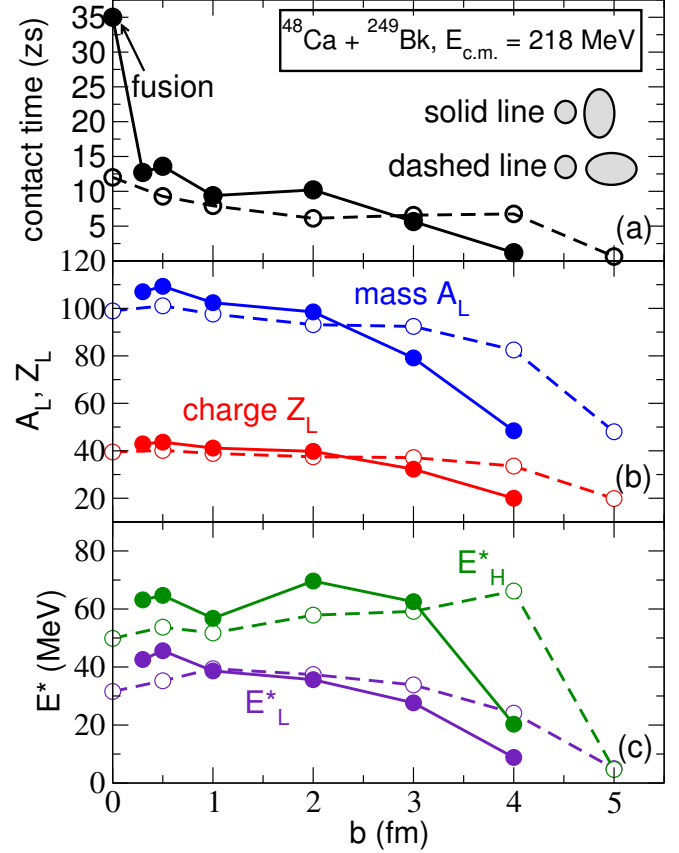

FIG. 7. (Color online) (a) Contact time, (b) mass and charge of the light fragment, and (c) excitation energy E^* of the heavy and light fragments for ^{48}Ca $+^{249}$Bk as a function of impact parameter, calculated at $E_{c.m.} = 218$ MeV. The impact parameter labels on the horizontal axis correspond to orbital angular momentum values $L/\hbar = 0$, 21, 41, 62, 82, and 103, respectively

consider collisions of ^{48}Ca with the side of ^{249}Bk. Figure 7 (solid lines) shows that fusion is only observed in the narrow impact parameter region $b < 0.3$ fm, as evidenced by contact times exceeding 35 zs and a mononuclear shape without any neck formation. Quasifission reactions with contact times of $5.6-13.6$ zs are found at impact parameters $b = 0.3-3.0$ fm, with light fragment masses $A_L = 80-109$ and excitation energies $E_L^* = 28-45$ MeV. Impact parameters $b > 4$ fm yield deep-inelastic collisions (DIC), multi-nucleon transfer and inelastic collisions.

It is interesting to note the atypical rise of the contact time between impact parameters $b = 1$ fm and $b = 2$ fm, see Fig. 7 (a). As shown in Fig. 7 (b), for these impact parameters the light fragment is in the region of the neutron rich ^{100}Zr isotope. The microscopic evolution of the shell structure seems to have a tendency to form a composite with a longer life-
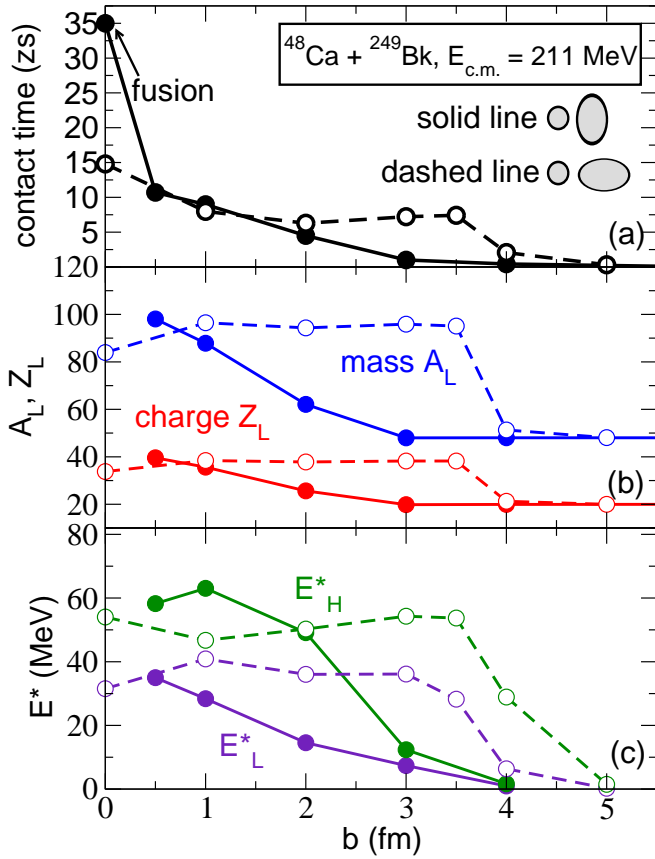
FIG. 8. (Color online) Same as Fig. 7, but calculated at a lower energy $E_{c.m.} = 211$ MeV. The impact parameter labels on the horizontal axis correspond to orbital angular momentum values $L/\hbar = 0, 20, 40, 61, 81$, and 101, respectively
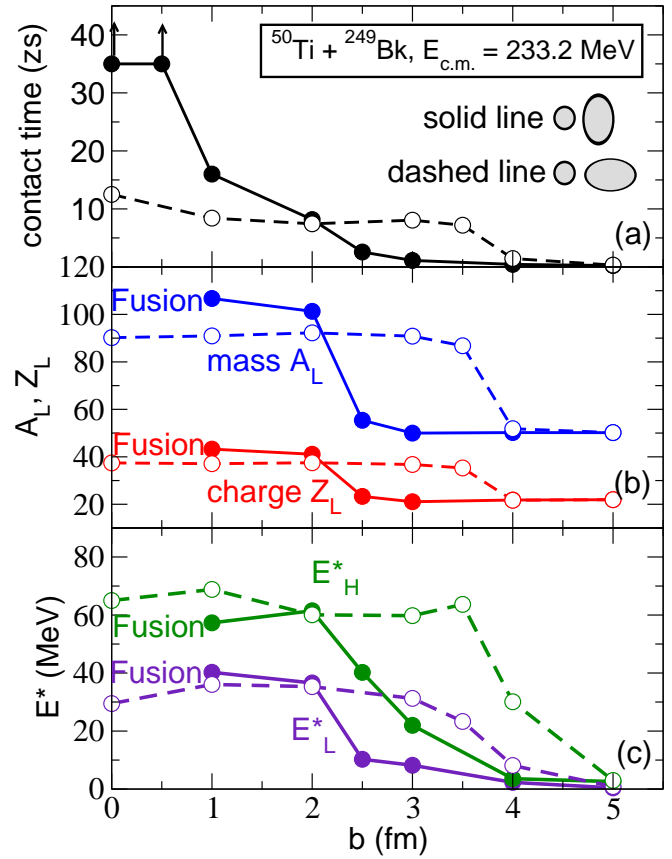
FIG. 9. (Color online) (a) Contact time, (b) mass and charge of the light fragment, and (c) excitation energy E^* of the heavy and light fragments for ^{50}Ti + ^{249}Bk as a function of impact parameter, calculated at $E_{c.m.} = 233.2$ MeV. The impact parameter labels on the horizontal axis correspond to orbital angular momentum values $L/\hbar = 0, 22, 43, 65, 87$, and 108, respectively.

time when the light fragment is in this region. This was also discussed for the case of ^{40,48}Ca+^{238}U quasifission study of Ref. [104]. In Ref. [104] this was explained as being due to the presence of strongly bound deformed isotopes of Zr in this region [128, 129].

Next we consider collisions of ^{48}Ca with the tip of ^{249}Bk (dashed lines in Fig. 7). No fusion events are found for this initial orientation. Quasifission reactions with contact times of $6-12$ zs are found at impact parameters $b = 0 - 4$ fm, with light fragment masses $A_L = 82 - 101$ and excitation energies $E_L^* = 24 - 39$ MeV. Impact parameters $b > 5$ fm yield DIC, multi-nucleon transfer and inelastic collisions.

We have repeated these calculations at a lower center-of-mass energy of $E_{c.m.} = 211$ MeV. The results are shown in Figure 8. For the tip orientation, all observables are quite similar to those obtained at $E_{c.m.} = 218$ MeV. However, for the side orientation, we find that the contact time decreases more rapidly with impact parameter than at higher energy. As a result, both mass transfer and fragment excitation energies also decrease faster. Fusion is found for impact parameters $b < 0.5$ fm (for the side orientation of ^{249}Bk only).

Figure 9 shows results for the ^{50}Ti + ^{249}Bk system at $E_{c.m.} = 233.2$ MeV as a function of impact parameter. Let us first consider collisions with the side of ^{249}Bk (solid lines).

Fusion is observed at impact parameters $b = 0$ fm and $b = 0.5$ fm. Quasifission reactions with contact times of $8 - 16$ zs are found at impact parameters $b = 1$ fm and at $b = 2$ fm, with light fragment masses $A_L = 101 - 107$ and excitation energies $E_L^* = 36 - 40$ MeV. Impact parameters $b > 2.5$ fm yield DIC, multi-nucleon transfer and inelastic collisions.

Now we consider collisions with the tip of ^{249}Bk (dashed lines). No fusion events are found for this initial orientation. Quasifission reactions with contact times of $7.4 - 12.5$ zs are found at impact parameters $b = 0 - 3$ fm, with light fragment masses $A_L = 90 - 92$ and excitation energies $E_L^* = 29 - 36$ MeV. Impact parameters $b > 3.5$ fm produce DIC, multi-nucleon transfer, and inelastic collisions.

Experiments at Dubna and at GSI-TASCA have produced several isotopes of superheavy element 117 with cross-sections of $2-3$ picobarns in the reaction ^{48}Ca +^{249}Bk. However, attempts to synthesize isotopes of element 119 in the reaction ^{50}Ti +^{249}Bk have been unsuccessful so far. One possible reason could be different excitation energies in these systems. In order to investigate this conjecture, we have calculated the total excitation energy for both systems as a function of impact parameter. This quantity can be calculated with

the DC-TDHF method for both fusion and quasifission. The results are displayed in Figure 10 for the side orientation of ^{249}Bk. The total excitation energy is shown as a function of
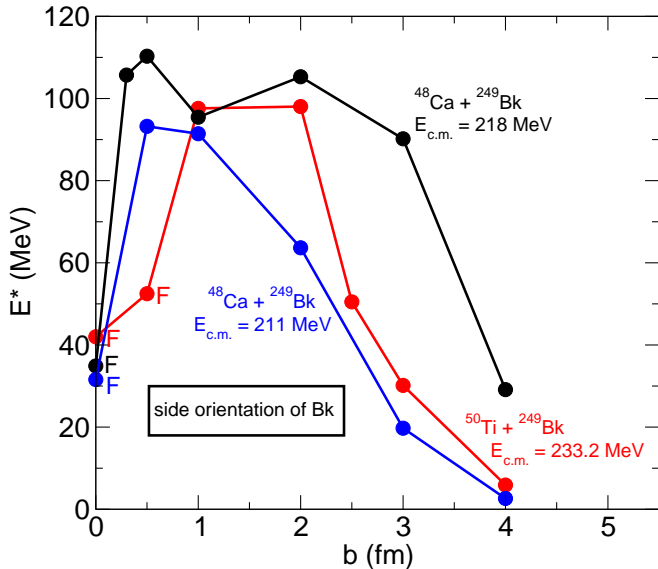

FIG. 10. (Color online) Comparison of the total excitation energy for the systems ^{48}Ca $+^{249}$Bk and ^{50}Ti $+^{249}$Bk (side orientation) as a function of impact parameter. The points corresponding to fusion events are indicated by a letter F.

impact parameter for the ^{48}Ca $+^{249}$Bk system at two center-of-mass energies, $E_{c.m.} = 211$ MeV and $E_{c.m.} = 218$ MeV. Naturally, the excitation energy increases with increasing $E_{c.m.}$. Also shown is the total excitation energy of ^{50}Ti $+^{249}$Bk, calculated at the GSI-TASCA energy of $E_{c.m.} = 233.2$ MeV. The most important region is the region of small impact parameters where fusion occurs (for the side orientation of ^{249}Bk only). We find the interesting result that the total excitation energy of both systems is almost identical at impact parameters $b = 0$ fm (fusion) and $b = 1$ fm (QF). For impact parameters $b > 1.5$ fm, the total excitation energy of the ^{50}Ti $+^{249}$Bk system is found to be in between the two curves calculated for ^{48}Ca $+^{249}$Bk. We conclude that the excitation energy of the fused system or of the quasifission fragments does not exhibit strong differences between ^{48}Ca and ^{50}Ti induced reactions.

E. Mass-angle distributions

In this section we study mass-angle distributions (MADs) arising from quasifission. MADs have proven to be an efficient experimental tool to understand quasifission dynamics and how this mechanism is affected by the structure of the reactants [25–27, 36, 40, 42–48, 130–133]. TDHF calculations can help the analysis and interpretation of experimental MADs [42, 45, 46, 48].

The MAD is obtained by plotting the scattering angle $\theta_{c.m.}$ as a function of the mass ratio $M_R = m_1/(m_1 + m_2)$ where m_1 and m_2 are the masses of the fission-like fragments. In Fig. 11 we show TDHF calculations of mass-angle distribu-

tions for ^{48}Ca $+^{249}$Bk at $E_{c.m.} = 218$ MeV. The MAD regions
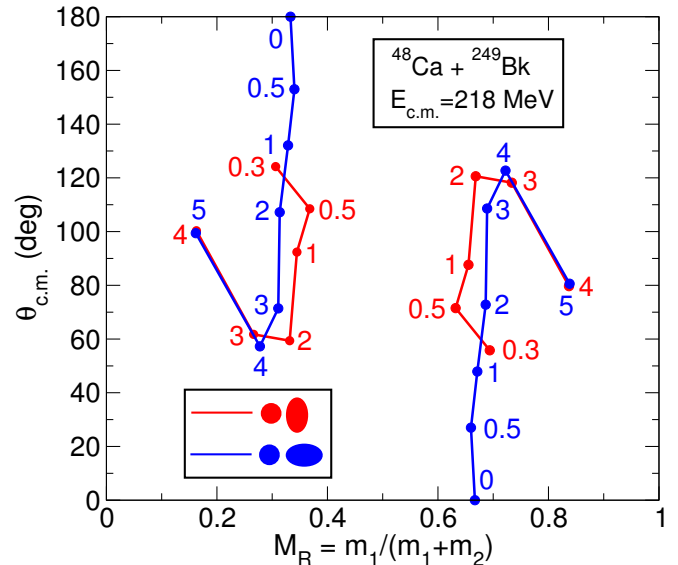

FIG. 11. (Color online) Mass-angle distribution for the ^{48}Ca $+^{249}$Bk system at $E_{c.m.} = 218$ MeV, calculated for tip and side orientations of the ^{249}Bk nucleus. The impact parameters (in units of fm) are indicated by the numbers next to each data point.

near $M_R = 0.16$ and $M_R = 0.84$ correspond to quasielastic and deep-inelastic reactions. In the region $0.25 < M_R < 0.75$ fission-like fragments are observed.

For the quasifission events which occur at time scales between 5.6 zs and 13.6 zs, our TDHF calculations show a strong correlation between scattering angle and mass ratio. The reason for this correlation is that the mass transfer between the two fragments increases with the rotation (contact) time (see Figure 7a,b) which in turn impacts the scattering angle. Hence, the MADs for quasifission events can be used as a clock for the rotation period of the system [25, 27].

For the tip orientation of the ^{249}Bk nucleus (blue curve in Fig. 11) TDHF shows quasifission at impact parameters $b = 0 - 4$ fm and a deep-inelastic reaction at $b = 5$ fm. No fusion events are predicted by TDHF for the tip orientation. On the other hand, for the side orientation of the ^{249}Bk nucleus (red curve) the TDHF calculations show fusion at impact parameter $b = 0$ fm, quasifission at impact parameters $b = 0.3 - 3.0$ fm, and a deep-inelastic reaction at $b = 4$ fm. In general, collisions with the side of ^{249}Bk yield an increase in the mass ratio for quasifission. The maximum value for the light fragment, $M_R = 0.368$, is obtained at impact parameter $b = 0.5$ fm. Note that as a result of the single-Slater-determinant approximation, TDHF is a deterministic theory that will provide us only with the most probable reaction products for the MADs rather than with the full mass distribution.

In fusion-fission reactions a compound nucleus is formed which subsequently decays by fission at a time-scale that is much longer than observed in quasifission, with no memory of the entrance channel and therefore no mass-angle correlation. In experiments, fission fragments are usually more symmetric than in quasifission, producing a peak around $M_R = 0.5$. Even

though our TDHF calculations predict fusion for the small impact parameter range $b < 0.3$ fm (and only for the side orientation of the ^{249}Bk nucleus), it is not possible to obtain a fully equilibrated nucleus undergoing fission in TDHF calculations because of limitations of the mean-field approach.

In Fig. 12 we show TDHF calculations of the mass-angle distribution for the same system, but at a lower energy $E_{c.m.} = 211$ MeV. The MAD for the tip orientation of the ^{249}Bk nu-
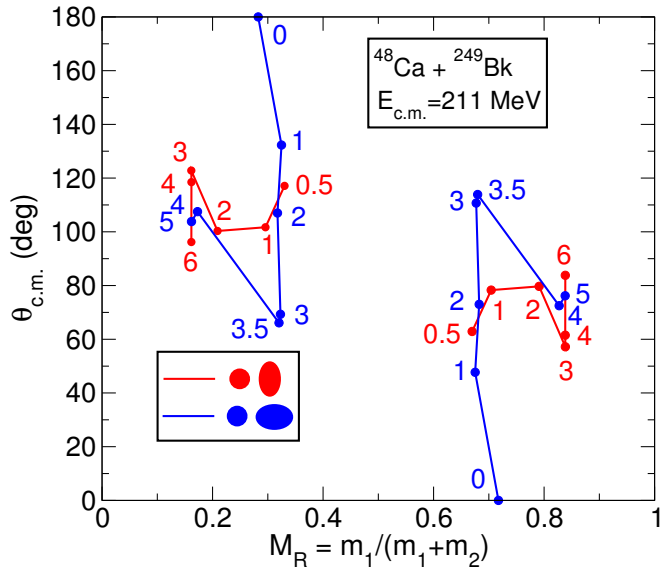

FIG. 12. (Color online) Same as Fig. 11, but at a lower energy $E_{c.m.} = 211$ MeV.

cleus (blue curve) looks quite similar to the one obtained at higher energy. However, for the side orientation (red curve) we find a different mass-angle distribution: the scattering angles for the light fragment are confined to a small region $\theta_{c.m.} = 96 - 123$ deg, and the fragments are more asymmetric than at $E_{c.m.} = 218$ MeV.

In Fig. 13 we show TDHF calculations of quasifission mass-angle distributions for ^{50}Ti$+^{249}$Bk at $E_{c.m.} = 233$ MeV, corresponding to the two orientations of the ^{249}Bk nucleus. The MAD for the tip orientation (blue curve) are very similar to the result obtained for ^{48}Ca$+^{249}$Bk at $E_{c.m.} = 218$ MeV (see Fig. 11). The MAD for the side orientation (red curve) also shows similarities with the ^{48}Ca induced one at 218 MeV, with fragments produced in a similar angular range ($60 - 120$ deg.) and with a maximum M_R for the light fragment extending almost to 0.4. In the details, however, differences are observed on the position in the MADs of events associated with specific impact parameters.

F. Mass-TKE distributions

Correlations between mass and total kinetic energy (TKE) of the fragments have often been measured in experimental studies of quasifission [25, 26, 31, 34, 35, 38, 39, 51, 134, 135]. Plots of fragment mass versus TKE are often used to separate quasi-elastic events to fully damped events such
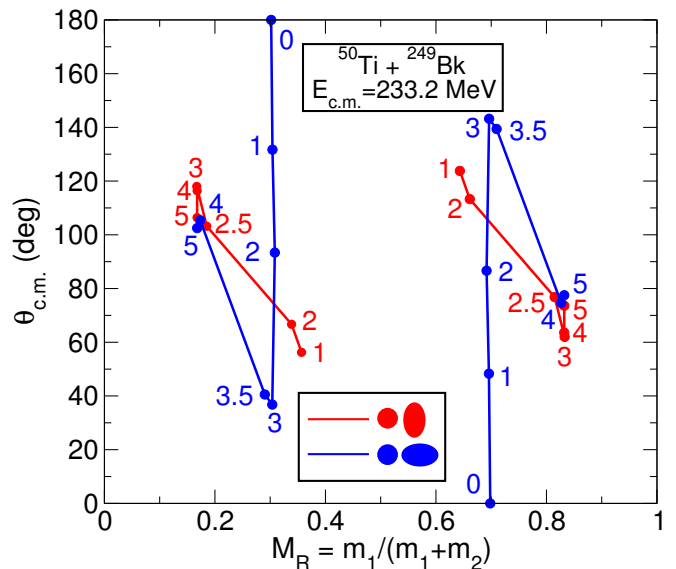

FIG. 13. (Color online) Mass-angle distribution for ^{50}Ti$+^{249}$Bk at $E_{c.m.} = 233$ MeV, calculated for tip and side orientations of the ^{249}Bk nucleus. The impact parameters (in units of fm) are indicated by the numbers next to each data point.

as quasifission and fusion-fission. In between, deep-inelastic collisions are characterized by a partial damping of the initial kinetic energy and a relatively small (compared to quasifission) mass transfer. Fully damped events are expected to have a TKE close to the Viola systematics for fission fragments [136, 137].

In TDHF, the TKE of the fragments is simply obtained from the exit channel of the collision. For well separated fragments, it is straightforward to compute the kinetic energy of each fragment ($i = 1, 2$) at time t according to

$$T_i(t) = \frac{1}{2}M_i \left(\frac{dR_i(t)}{dt} \right)^2,$$

where M_i is the final mass of the fragment i (neglecting nucleon emission) and R_i its distance from the center of mass of the total system. Although the fragments do not interact anymore via the strong nuclear interaction, they are close enough feel the Coulomb repulsion from the other fragment. The TKE is then estimated by the sum of the kinetic energy of the fragments after their separation and their Coulomb potential energy assuming that the fragments are point like charges,

$$TKE \simeq T_1(t) + T_2(t) + \frac{Z_1 Z_2 e^2}{R(t)},$$

where $R(t) = R_1(t) + R_2(t)$.

Figures 14(a) and (b) show a compilation of the mass-TKE distributions obtained in ^{48}Ca,^{50}Ti$+^{249}$Bk TDHF calculations, respectively. The figures also show the TKE expected from the Viola systematics accounting for fragment mass asymmetry [137] and assuming that the fragments have the same N/Z ratio as the compound nucleus (dashed lines). Overall, we observe that the TKE are distributed around the
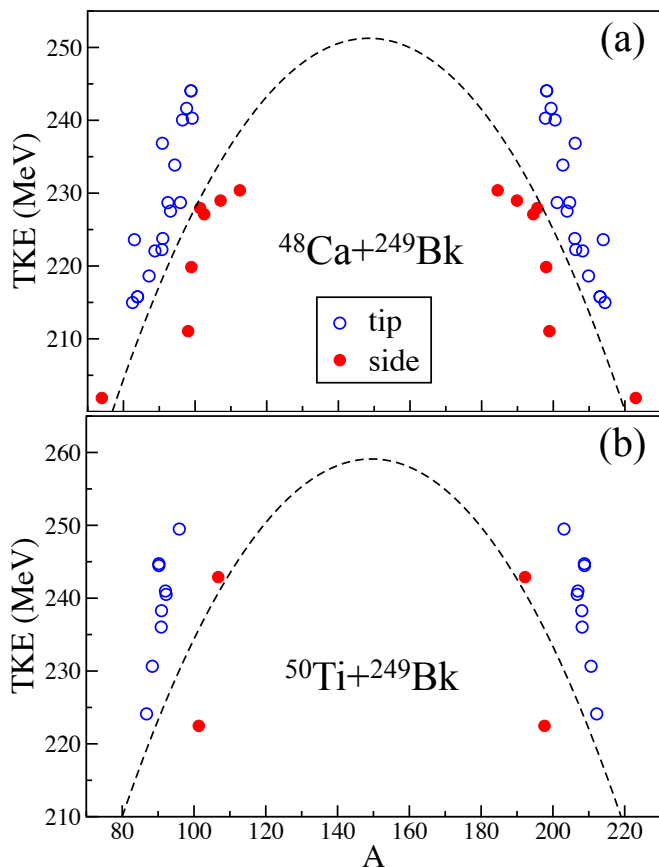
FIG. 14. (Color online) TKE-mass correlations in (a) ^{48}Ca$+^{249}$Bk and (b) ^{50}Ti$+^{249}$Bk. Tip (side) orientations are plotted with open (filled) symbols. The dashed line is the Viola systematics assuming that the fragments have the neutron-to-proton ratio of the compound nucleus.
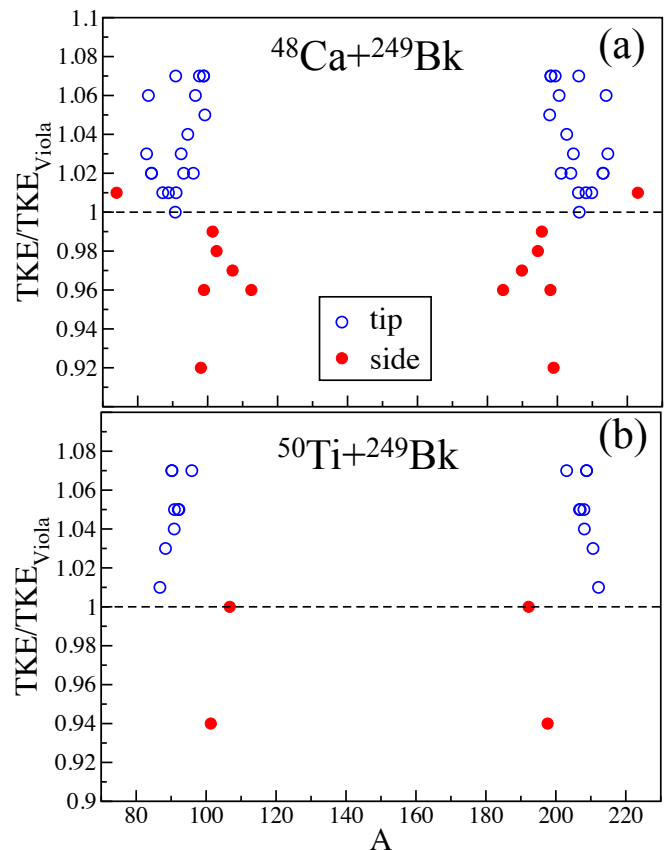
FIG. 15. (Color online) Same as Fig. 14 but with the TKE normalized to the TKE from Viola systematics using the masses and charges of the fragments in the exit channel.

IV. CONCLUSIONS

The Time-Dependent Hartree-Fock (TDHF) theory provides a dynamic quantum many-body description of nuclear reactions. The only input is the effective nucleon-nucleon interaction (Skyrme) which is fitted to the static properties of a few nuclei, otherwise there are no adjustable parameters. TDHF has proven to be a valuable tool for elucidating some of the underlying physics of heavy-ion reactions in the vicinity of the Coulomb barrier. In this paper, we have studied the transition between various reaction mechanisms including fusion, quasifission, deep-inelastic collisions, and quasi-elastic reactions in collisions of ^{48}Ca$+^{249}$Bk and ^{50}Ti$+^{249}$Bk which have been used to synthesize elements $Z = 117, 119$. Quasifission is the primary reaction mechanism that limits the formation of superheavy nuclei.

In addition, heavy-ion interaction potentials are obtained with the Density-Constrained Time-Dependent Hartree-Fock (DC-TDHF) method. Because of the prolate deformation of the Bk nucleus, these potentials (and other observables) depend strongly on the relative orientation of ^{249}Bk. In particular, we present results for the "tip" and "side" orientation. Using TDHF, we calculate nuclear contact times, masses and charges of the two fragments, and their pre-compound excitation energies. Specifically, we study the energy-dependence

Viola estimates, indicating that most of the relative kinetic energy has been dissipated in the collision. However, the distributions associated with side and tip orientations are well separated, with the side (tip) collisions leading essentially to a TKE below (above) the Viola systematics.

One could argue that assuming that the fragments have the same N/Z as the compound nucleus is a crude approximation, in particular for systems with large asymmetry in the exit channels as observed here. Therefore, we have also computed the TKE according to the Viola estimate using the masses and charges of the fragments in the exit channel obtained from TDHF. The results are plotted in Figs. 15(a) and (b) which show the ratio of the TDHF final TKE over the TKE from Viola estimate with TDHF mass and charge partitions. The previous conclusion are still valid, i.e., the tip (side) orientations are associated with more (less) final TKE than the Viola systematics. This means that less damping occurs in collisions with the tip than with the side. This conclusion, however, does not depend on if the projectile is a ^{48}Ca or a ^{50}Ti, indicating again that the reaction dynamics is relatively similar in both systems.

of these quantities for central collisions, and we calculate the impact parameter dependence at selected fixed energies. Finally, we present results for mass-angle and mass-TKE distributions. The orientation of the actinide plays a crucial role on these observables.

In agreement with experiments at Dubna and at GSI-TASCA, our TDHF and DC-TDHF calculations predict fusion in the reactions ^{48}Ca $+^{249}$Bk resulting in isotopes of element 117. While experimental attempts at GSI-TASCA to synthesize element 119 in the reaction ^{50}Ti $+^{249}$Bk have so far not been successful, the TDHF calculations do find fusion in this system also. In fact, our calculations do not show significantly different behaviors of the entrance channel dynamics between the two projectiles.

[1] M. Bender, K. Rutz, P.-G. Reinhard, J. A. Maruhn, and W. Greiner, Phys. Rev. C **60**, 034304 (1999).

[2] M. Bender, W. Nazarewicz, and P.-G. Reinhard, Phys. Lett. B **515**, 42 (2001).

[3] W. Nazarewicz, M. Bender, S. Ćwiok, P. Heenen, A. Kruppa, P.-G. Reinhard, and T. Vertse, Nucl. Phys. A **701**, 165 (2002).

[4] S. Ćwiok, P.-H. Heenen, and W. Nazarewicz, Nature **433**, 705 (2005).

[5] J. C. Pei, F. R. Xu, and P. D. Stevenson, Phys. Rev. C **71**, 034302 (2005).

[6] J. C. Pei, W. Nazarewicz, J. A. Sheikh, and A. K. Kerman, Phys. Rev. Lett. **102**, 192501 (2009).

[7] S. Hofmann and G. Münzenberg, Rev. Mod. Phys. **72**, 733 (2000).

[8] S. Hofmann, F. P. Heßberger, D. Ackermann, G. Münzenberg, S. Antalic, P. Cagarda, B. Kindler, J. Kojouharova, M. Leino, B. Lommel, R. Mann, A. G. Popeko, S. Reshitko, S. Śaro, J. Uusitalo, and A. V. Yeremin, Eur. Phys. J. A **14**, 147 (2002).

[9] G. Münzenberg and K. Morita, Nucl. Phys. A **944**, 3 (2015).

[10] K. Morita, Nucl. Phys. A **944**, 30 (2015).

[11] S. Hofmann, S. Heinz, R. Mann, J. Maurer, G. Münzenberg, S. Antalic, W. Barth, H. G. Burkhard, L. Dahl, K. Eberhardt, R. Grzywacz, J. H. Hamilton, R. A. Henderson, J. M. Kenneally, B. Kindler, I. Kojouharov, R. Lang, B. Lommel, K. Miernik, D. Miller, K. J. Moody, K. Morita, K. Nishio, A. G. Popeko, J. B. Roberto, J. Runke, K. P. Rykaczewski, S. Saro, C. Scheidenberger, H. J. Schött, D. A. Shaughnessy, M. A. Stoyer, P. Thörle-Pospiech, K. Tinschert, N. Trautmann, J. Uusitalo, and A. V. Yeremin, Eur. Phys. J. A **52**, 180 (2016).

[12] Y. Oganessian, J. Phys. G **34**, R165 (2007).

[13] Yu. Ts. Oganessian, F. Sh. Abdullin, P. D. Bailey, D. E. Benker, M. E. Bennett, S. N. Dmitriev, J. G. Ezold, J. H. Hamilton, R. A. Henderson, M. G. Itkis, Y. V. Lobanov, A. N. Mezentsev, K. J. Moody, S. L. Nelson, A. N. Polyakov, C. E. Porter, A. V. Ramayya, F. D. Riley, J. B. Roberto, M. A. Ryabinin, K. P. Rykaczewski, R. N. Sagaidak, D. A. Shaughnessy, I. V. Shirokovsky, M. A. Stoyer, V. G. Subbotin, R. Sudowe, A. M. Sukhov, Y. S. Tsyganov, V. K. Utyonkov, A. A. Voinov, G. K. Vostokin, and P. A. Wilk, Phys. Rev. Lett. **104**, 142502 (2010).

[14] Y. T. Oganessian, F. S. Abdullin, C. Alexander, J. Binder, R. A. Boll, S. N. Dmitriev, J. Ezold, K. Felker, J. M. Gostic, R. K. Grzywacz, J. H. Hamilton, R. A. Henderson, M. G. Itkis, K. Miernik, D. Miller, K. J. Moody, A. N. Polyakov, A. V. Ramayya, J. B. Roberto, M. A. Ryabinin, K. P. Rykaczewski, R. N. Sagaidak, D. A. Shaughnessy, I. V. Shirokovsky, M. V. Shumeiko, M. A. Stoyer, N. J. Stoyer, V. G. Subbotin, A. M. Sukhov, Y. S. Tsyganov, V. K. Utyonkov, A. A. Voinov, and G. K. Vostokin, Phys. Rev. C **87**, 054621 (2013).

[15] J. B. Roberto, C. W. Alexander, R. A. Boll, J. D. Burns, J. G. Ezold, L. K. Felker, S. L. Hogle, and K. P. Rykaczewski, Nucl. Phys. A **944**, 99 (2015).

[16] Yu. Ts. Oganessian and V. Utyonkov, Nucl. Phys. A **944**, 62 (2015).

[17] S. Hofmann, D. Ackermann, S. Antalic, H. G. Burkhard, V. F. Comas, R. Dressler, Z. Gan, S. Heinz, J. A. Heredia, F. P. Heßberger, J. Khuyagbaatar, B. Kindler, I. Kojouharov, P. Kuusiniemi, M. Leino, B. Lommel, R. Mann, G. Münzenberg, K. Nishio, A. G. Popeko, S. Saro, H. J. Schött, B. Streicher, B. Sulignano, J. Uusitalo, M. Venhart, and A. V. Yeremin, Eur. Phys. J. A **32**, 251 (2007).

[18] L. Stavsetra, K. E. Gregorich, J. Dvorak, P. A. Ellison, I. Dragojević, M. A. Garcia, and H. Nitsche, Phys. Rev. Lett. **103**, 132502 (2009).

[19] C. E. Düllmann, M. Schädel, A. Yakushev, A. Türler, K. Eberhardt, J. V. Kratz, D. Ackermann, L.-L. Andersson, M. Block, W. Brüchle, J. Dvorak, H. G. Essel, P. A. Ellison, J. Even, J. M. Gates, A. Gorshkov, R. Graeger, K. E. Gregorich, W. Hartmann, R.-D. Herzberg, F. P. Heßberger, D. Hild, A. Hübner, E. Jäger, J. Khuyagbaatar, B. Kindler, J. Krier, N. Kurz, S. Lahiri, D. Liebe, B. Lommel, M. Maiti, H. Nitsche, J. P. Omtvedt, E. Parr, D. Rudolph, J. Runke, B. Schausten, E. Schimpf, A. Semchenkov, J. Steiner, P. Thörle-Pospiech, J. Uusitalo, M. Wegrzecki, and N. Wiehl, Phys. Rev. Lett. **104**, 252701 (2010).

[20] Hofmann, S., Heinz, S., Mann, R., Maurer, J., Khuyagbaatar, J., Ackermann, D., Antalic, S., Barth, W., Block, M., Burkhard, H. G., Comas, V. F., Dahl, L., Eberhardt, K., Gostic, J., Henderson, R. A., Heredia, J. A., Heßberger, F. P., Kenneally, J. M., Kindler, B., Kojouharov, I., Kratz, J. V., Lang, R., Leino, M., Lommel, B., Moody, K. J., Münzenberg, G., Nelson, S. L., Nishio, K., Popeko, A. G., Runke, J., Saro, S., Shaughnessy, D. A., Stoyer, M. A., Thörle-Pospiech, P., Tinschert, K., Trautmann, N., Uusitalo, J., Wilk, P. A., and Yeremin, A. V., Eur. Phys. J. A **48**, 62 (2012).

[21] D. Rudolph, U. Forsberg, P. Golubev, L. G. Sarmiento, A. Yakushev, L.-L. Andersson, A. Di Nitto, C. E. Düllmann, J. M. Gates, K. E. Gregorich, C. J. Gross, F. P. Heßberger, R.-D. Herzberg, J. Khuyagbaatar, J. V. Kratz, K. Rykaczewski, M. Schädel, S. Åberg, D. Ackermann,

M. Block, H. Brand, B. G. Carlsson, D. Cox, X. Derkx, K. Eberhardt, J. Even, C. Fahlander, J. Gerl, E. Jäger, B. Kindler, J. Krier, I. Kojouharov, N. Kurz, B. Lommel, A. Mistry, C. Mokry, H. Nitsche, J. P. Omtvedt, P. Papadakis, I. Ragnarsson, J. Runke, H. Schaffner, B. Schausten, P. Thörle-Pospiech, T. Torres, T. Traut, N. Trautmann, A. Türler, A. Ward, D. E. Ward, and N. Wiehl, Phys. Rev. Lett. **111**, 112502 (2013).

[22] J. Khuyagbaatar, A. Yakushev, C. E. Düllmann, D. Ackermann, L.-L. Andersson, M. Asai, M. Block, R. A. Boll, H. Brand, D. M. Cox, M. Dasgupta, X. Derkx, A. Di Nitto, K. Eberhardt, J. Even, M. Evers, C. Fahlander, U. Forsberg, J. M. Gates, N. Gharibyan, P. Golubev, K. E. Gregorich, J. H. Hamilton, W. Hartmann, R.-D. Herzberg, F. P. Heßberger, D. J. Hinde, J. Hoffmann, R. Hollinger, A. Hübner, E. Jäger, B. Kindler, J. V. Kratz, J. Krier, N. Kurz, M. Laatiaoui, S. Lahiri, R. Lang, B. Lommel, M. Maiti, K. Miernik, S. Minami, A. Mistry, C. Mokry, H. Nitsche, J. P. Omtvedt, G. K. Pang, P. Papadakis, D. Renisch, J. Roberto, D. Rudolph, J. Runke, K. P. Rykaczewski, L. G. Sarmiento, M. Schädel, B. Schausten, A. Semchenkov, D. A. Shaughnessy, P. Steinegger, J. Steiner, E. E. Tereshatov, P. Thörle-Pospiech, K. Tinschert, T. Torres De Heidenreich, N. Trautmann, A. Türler, J. Uusitalo, D. E. Ward, M. Wegrzecki, N. Wiehl, S. M. Van Cleve, and V. Yakusheva, Phys. Rev. Lett. **112**, 172501 (2014).

[23] C. E. Düllmann and the TASCA collaboration, in *Fission and Properties of Neutron-Rich Nuclei*, Vol. 44 (World Scientific, 2013) pp. 271–277.

[24] R. Bock, Y. T. Chu, M. Dakowski, A. Gobbi, E. Grosse, A. Olmi, H. Sann, D. Schwalm, U. Lynen, W. Müller, S. Bjørnholm, H. Esbensen, W. Wölfli, and E. Morenzoni, Nucl. Phys. A **388**, 334 (1982).

[25] J. Töke, R. Bock, G. X. Dai, A. Gobbi, S. Gralla, K. D. Hildenbrand, J. Kuzminski, W. F. J. Müller, A. Olmi, H. Stelzer, B. B. Back, and S. Bjørnholm, Nucl. Phys. A **440**, 327 (1985).

[26] W. Q. Shen, J. Albinski, A. Gobbi, S. Gralla, K. D. Hildenbrand, N. Herrmann, J. Kuzminski, W. F. J. Müller, H. Stelzer, J. Töke, B. B. Back, S. Bjørnholm, and S. P. Sørensen, Phys. Rev. C **36**, 115 (1987).

[27] R. du Rietz, D. J. Hinde, M. Dasgupta, R. G. Thomas, L. R. Gasques, M. Evers, N. Lobanov, and A. Wakhle, Phys. Rev. Lett. **106**, 052701 (2011).

[28] C.-C. Sahm, H.-G. Clerc, K.-H. Schmidt, W. Reisdorf, P. Armbruster, F. P. Heßberger, J. G. Keller, G. Münzenberg, and D. Vermeulen, Z. Phys. A **319**, 113 (1984).

[29] H. Gäggeler, T. Sikkeland, G. Wirth, W. Brüchle, W. Bögl, G. Franz, G. Herrmann, J. V. Kratz, M. Schädel, K. Sümmerer, and W. Weber, Z. Phys. A **316**, 291 (1984).

[30] K.-H. Schmidt and W. Morawek, Rep. Prog. Phys. **54**, 949 (1991).

[31] D. J. Hinde, D. Hilscher, H. Rossner, B. Gebauer, M. Lehmann, and M. Wilpert, Phys. Rev. C **45**, 1229 (1992).

[32] D. J. Hinde, M. Dasgupta, J. R. Leigh, J. P. Lestone, J. C. Mein, C. R. Morton, J. O. Newton, and H. Timmers, Phys. Rev. Lett. **74**, 1295 (1995).

[33] D. J. Hinde, M. Dasgupta, J. R. Leigh, J. C. Mein, C. R. Morton, J. O. Newton, and H. Timmers, Phys. Rev. C **53**, 1290 (1996).

[34] M. G. Itkis, J. Äystö, S. Beghini, A. A. Bogachev, L. Corradi, O. Dorvaux, A. Gadea, G. Giardina, F. Hanappe, I. M. Itkis, M. Jandel, J. Kliman, S. V. Khlebnikov, G. N. Kniajeva, N. A. Kondratiev, E. M. Kozulin, L. Krupa, A. Latina, T. Materna, G. Montagnoli, Y. T. Oganessian, I. V. Pokrovsky, E. V.

Prokhorova, N. Rowley, V. A. Rubchenya, A. Y. Rusanov, R. N. Sagaidak, F. Scarlassara, A. M. Stefanini, L. Stuttge, S. Szilner, M. Trotta, W. H. Trzaska, D. N. Vakhtin, A. M. Vinodkumar, V. M. Voskressenski, and V. I. Zagrebaev, Nucl. Phys. A **734**, 136 (2004).

[35] G. N. Knyazheva, E. M. Kozulin, R. N. Sagaidak, A. Y. Chizhov, M. G. Itkis, N. A. Kondratiev, V. M. Voskressensky, A. M. Stefanini, B. R. Behera, L. Corradi, E. Fioretto, A. Gadea, A. Latina, S. Szilner, M. Trotta, S. Beghini, G. Montagnoli, F. Scarlassara, F. Haas, N. Rowley, P. R. S. Gomes, and A. Szanto de Toledo, Phys. Rev. C **75**, 064602 (2007).

[36] D. J. Hinde, R. G. Thomas, R. du Rietz, A. Diaz-Torres, M. Dasgupta, M. L. Brown, M. Evers, L. R. Gasques, R. Rafiei, and M. D. Rodriguez, Phys. Rev. Lett. **100**, 202701 (2008).

[37] K. Nishio, H. Ikezoe, S. Mitsuoka, I. Nishinaka, Y. Nagame, Y. Watanabe, T. Ohtsuki, K. Hirose, and S. Hofmann, Phys. Rev. C **77**, 064607 (2008).

[38] E. M. Kozulin, G. N. Knyazheva, S. N. Dmitriev, I. M. Itkis, M. G. Itkis, T. A. Loktev, K. V. Novikov, A. N. Baranov, W. H. Trzaska, E. Vardaci, S. Heinz, O. Beliuskina, and S. V. Khlebnikov, Phys. Rev. C **89**, 014614 (2014).

[39] I. M. Itkis, E. M. Kozulin, M. G. Itkis, G. N. Knyazheva, A. A. Bogachev, E. V. Chernysheva, L. Krupa, Y. T. Oganessian, V. I. Zagrebaev, A. Y. Rusanov, F. Goennenwein, O. Dorvaux, L. Stuttgé, F. Hanappe, E. Vardaci, and E. Goés de Brennand, Phys. Rev. C **83**, 064613 (2011).

[40] C. J. Lin, R. du Rietz, D. J. Hinde, M. Dasgupta, R. G. Thomas, M. L. Brown, M. Evers, L. R. Gasques, and M. D. Rodriguez, Phys. Rev. C **85**, 014611 (2012).

[41] K. Nishio, S. Mitsuoka, I. Nishinaka, H. Makii, Y. Wakabayashi, H. Ikezoe, K. Hirose, T. Ohtsuki, Y. Aritomo, and S. Hofmann, Phys. Rev. C **86**, 034608 (2012).

[42] C. Simenel, D. J. Hinde, R. du Rietz, M. Dasgupta, M. Evers, C. J. Lin, D. H. Luong, and A. Wakhle, Phys. Lett. B **710**, 607 (2012).

[43] R. du Rietz, E. Williams, D. J. Hinde, M. Dasgupta, M. Evers, C. J. Lin, D. H. Luong, C. Simenel, and A. Wakhle, Phys. Rev. C **88**, 054618 (2013).

[44] E. Williams, D. J. Hinde, M. Dasgupta, R. du Rietz, I. P. Carter, M. Evers, D. H. Luong, S. D. McNeil, D. C. Rafferty, K. Ramachandran, and A. Wakhle, Phys. Rev. C **88**, 034611 (2013).

[45] A. Wakhle, C. Simenel, D. J. Hinde, M. Dasgupta, M. Evers, D. H. Luong, R. du Rietz, and E. Williams, Phys. Rev. Lett. **113**, 182502 (2014).

[46] K. Hammerton, Z. Kohley, D. J. Hinde, M. Dasgupta, A. Wakhle, E. Williams, V. E. Oberacker, A. S. Umar, I. P. Carter, K. J. Cook, J. Greene, D. Y. Jeung, D. H. Luong, S. D. McNeil, C. S. Palshetkar, D. C. Rafferty, C. Simenel, and K. Stiefel, Phys. Rev. C **91**, 041602 (2015).

[47] E. Prasad, D. J. Hinde, K. Ramachandran, E. Williams, M. Dasgupta, I. P. Carter, K. J. Cook, D. Y. Jeung, D. H. Luong, S. McNeil, C. S. Palshetkar, D. C. Rafferty, C. Simenel, A. Wakhle, J. Khuyagbaatar, C. E. Düllmann, B. Lommel, and B. Kindler, Phys. Rev. C **91**, 064605 (2015).

[48] E. Prasad, A. Wakhle, D. J. Hinde, E. Williams, M. Dasgupta, M. Evers, D. H. Luong, G. Mohanto, C. Simenel, and K. Vo-Phuoc, Phys. Rev. C **93**, 024607 (2016).

[49] M. Morjean, D. Jacquet, J. L. Charvet, A. L'Hoir, M. Laget, M. Parlog, A. Chbihi, M. Chevallier, C. Cohen, D. Dauvergne, R. Dayras, A. Drouart, C. Escano-Rodriguez, J. D. Frankland, R. Kirsch, P. Lautesse, L. Nalpas, C. Ray, C. Schmitt,

C. Stodel, L. Tassan-Got, E. Testa, and C. Volant, Phys. Rev. Lett. **101**, 072701 (2008).

[50] M. O. Frégeau, D. Jacquet, M. Morjean, E. Bonnet, A. Chbihi, J. D. Frankland, M. F. Rivet, L. Tassan-Got, F. Dechery, A. Drouart, L. Nalpas, X. Ledoux, M. Parlog, C. Ciortea, D. Dumitriu, D. Fluerasu, M. Gugiu, F. Gramegna, V. L. Kravchuk, T. Marchi, D. Fabris, A. Corsi, and S. Barlini, Phys. Rev. Lett. **108**, 122701 (2012).

[51] E. M. Kozulin, G. N. Knyazheva, I. M. Itkis, M. G. Itkis, A. A. Bogachev, L. Krupa, T. A. Loktev, S. V. Smirnov, V. I. Zagrebaev, J. Äystö, W. H. Trzaska, V. A. Rubchenya, E. Vardaci, A. M. Stefanini, M. Cinausero, L. Corradi, E. Fioretto, P. Mason, G. F. Prete, R. Silvestri, S. Beghini, G. Montagnoli, F. Scarlassara, F. Hanappe, S. V. Khlebnikov, J. Kliman, A. Brondi, A. Nitto, R. Moro, N. Gelli, and S. Szilner, Phys. Lett. B **686**, 227 (2010).

[52] G. Fazio, G. Giardina, G. Mandaglio, R. Ruggeri, A. I. Muminov, A. K. Nasirov, Y. T. Oganessian, A. G. Popeko, R. N. Sagaidak, A. V. Yeremin, S. Hofmann, F. Hanappe, and C. Stodel, Phys. Rev. C **72**, 064614 (2005).

[53] G. G. Adamian, N. V. Antonenko, and W. Scheid, Phys. Rev. C **68**, 034601 (2003).

[54] G. G. Adamian, N. V. Antonenko, and W. Scheid, Eur. Phys. J. A **41**, 235 (2009).

[55] A. K. Nasirov, G. Giardina, G. Mandaglio, M. Manganaro, F. Hanappe, S. Heinz, S. Hofmann, A. I. Muminov, and W. Scheid, Phys. Rev. C **79**, 024606 (2009).

[56] Zhao-Qing Feng, Gen-Ming Jin, Jun-Qing Li, and Werner Scheid, Nucl. Phys. A **816**, 33 (2009).

[57] A. Diaz Torres, G. G. Adamian, N. V. Antonenko, and W. Scheid, Nucl. Phys. A **679**, 410 (2001).

[58] V. I. Zagrebaev, Phys. Rev. C **64**, 034606 (2001).

[59] A. Diaz-Torres, G. G. Adamian, N. V. Antonenko, and W. Scheid, Phys. Rev. C **64**, 024604 (2001).

[60] Y. Aritomo and M. Ohta, Nucl. Phys. A **744**, 3 (2004).

[61] V. Zagrebaev and W. Greiner, J. Phys. G **31**, 825 (2005).

[62] A. Diaz-Torres, Phys. Rev. C **74**, 064601 (2006).

[63] R. Balian and M. Vénéroni, Phys. Rev. Lett. **47**, 1353 (1981).

[64] Roger Balian and Marcel Vénéroni, Phys. Lett. B **136**, 301 (1984).

[65] C. Simenel, Phys. Rev. Lett. **106**, 112502 (2011).

[66] D. Lacroix and S. Ayik, Eur. Phys. J. A **50**, 95 (2014).

[67] J. W. Negele, Rev. Mod. Phys. **54**, 913 (1982).

[68] C. Simenel, Eur. Phys. J. A **48**, 152 (2012).

[69] A. S. Umar and V. E. Oberacker, Phys. Rev. C **71**, 034314 (2005).

[70] J. A. Maruhn, P. G. Reinhard, P. D. Stevenson, J. Rikovska Stone, and M. R. Strayer, Phys. Rev. C **71**, 064328 (2005).

[71] T. Nakatsukasa and K. Yabana, Phys. Rev. C **71**, 024301 (2005).

[72] C. Simenel and P. Chomaz, Phys. Rev. C **68**, 024302 (2003).

[73] P.-G. Reinhard, P. D. Stevenson, D. Almehed, J. A. Maruhn, and M. R. Strayer, Phys. Rev. E **73**, 036709 (2006).

[74] P.-G. Reinhard, Lu Guo, and J. Maruhn, Eur. Phys. J. A **32**, 19 (2007).

[75] C. Simenel and P. Chomaz, Phys. Rev. C **80**, 064309 (2009).

[76] S. Fracasso, E. B. Suckling, and P. D. Stevenson, Phys. Rev. C **86**, 044303 (2012).

[77] C. I. Pardi and P. D. Stevenson, Phys. Rev. C **87**, 014330 (2013).

[78] C. I. Pardi, P. D. Stevenson, and K. Xu, Phys. Rev. E **89**, 033312 (2014).

[79] E. B. Suckling and P. D. Stevenson, EPL **90**, 12001 (2010).

[80] I. Stetcu, A. Bulgac, P. Magierski, and K. J. Roche, Phys. Rev.

C **84**, 051309 (2011).

[81] B. Avez and C. Simenel, Eur. Phys. J. A **49**, 76 (2013).

[82] G. Scamps and D. Lacroix, Phys. Rev. C **89**, 034314 (2014).

[83] P. Bonche, B. Grammaticos, and S. Koonin, Phys. Rev. C **17**, 1700 (1978).

[84] H. Flocard, S. E. Koonin, and M. S. Weiss, Phys. Rev. C **17**, 1682 (1978).

[85] C. Simenel, P. Chomaz, and G. de France, Phys. Rev. Lett. **86**, 2971 (2001).

[86] Kouhei Washiyama and Denis Lacroix, Phys. Rev. C **78**, 024610 (2008).

[87] A. S. Umar, V. E. Oberacker, J. A. Maruhn, and P.-G. Reinhard, Phys. Rev. C **81**, 064607 (2010).

[88] Lu Guo and Takashi Nakatsukasa, EPJ Web Conf. **38**, 09003 (2012).

[89] R. Keser, A. S. Umar, and V. E. Oberacker, Phys. Rev. C **85**, 044606 (2012).

[90] C. Simenel, R. Keser, A. S. Umar, and V. E. Oberacker, Phys. Rev. C **88**, 024617 (2013).

[91] V. E. Oberacker, A. S. Umar, J. A. Maruhn, and P.-G. Reinhard, Phys. Rev. C **85**, 034609 (2012).

[92] V. E. Oberacker, A. S. Umar, J. A. Maruhn, and P.-G. Reinhard, Phys. Rev. C **82**, 034603 (2010).

[93] A. S. Umar, V. E. Oberacker, and C. J. Horowitz, Phys. Rev. C **85**, 055801 (2012).

[94] C. Simenel, M. Dasgupta, D. J. Hinde, and E. Williams, Phys. Rev. C **88**, 064604 (2013).

[95] A. S. Umar, C. Simenel, and V. E. Oberacker, Phys. Rev. C **89**, 034611 (2014).

[96] X. Jiang, J. A. Maruhn, and S. Yan, Phys. Rev. C **90**, 064618 (2014).

[97] S. E. Koonin, K. T. R. Davies, V. Maruhn-Rezwani, H. Feldmeier, S. J. Krieger, and J. W. Negele, Phys. Rev. C **15**, 1359 (1977).

[98] C. Simenel, Phys. Rev. Lett. **105**, 192701 (2010).

[99] A. S. Umar, V. E. Oberacker, and J. A. Maruhn, Eur. Phys. J. A **37**, 245 (2008).

[100] Kazuyuki Sekizawa and Kazuhiro Yabana, Phys. Rev. C **88**, 014614 (2013).

[101] G. Scamps and D. Lacroix, Phys. Rev. C **87**, 014605 (2013).

[102] K. Sekizawa and K. Yabana, Phys. Rev. C **90**, 064614 (2014).

[103] D. Bourgin, C. Simenel, S. Courtin, and F. Haas, Phys. Rev. C **93**, 034604 (2016).

[104] V. E. Oberacker, A. S. Umar, and C. Simenel, Phys. Rev. C **90**, 054605 (2014).

[105] C. Simenel and A. S. Umar, Phys. Rev. C **89**, 031601 (2014).

[106] A. S. Umar, V. E. Oberacker, and C. Simenel, Phys. Rev. C **92**, 024621 (2015).

[107] A. S. Umar and V. E. Oberacker, Nucl. Phys. A **944**, 238 (2015).

[108] G. Scamps, C. Simenel, and D. Lacroix, Phys. Rev. C **92**, 011602 (2015).

[109] P. M. Goddard, P. D. Stevenson, and A. Rios, Phys. Rev. C **92**, 054610 (2015).

[110] A. Bulgac, P. Magierski, K. J. Roche, and I. Stetcu, Phys. Rev. Lett. **116**, 122504 (2016).

[111] K. Sekizawa and K. Yabana, Phys. Rev. C **93**, 054616 (2016).

[112] P.-G. Reinhard, A. S. Umar, K. T. R. Davies, M. R. Strayer, and S.-J. Lee, Phys. Rev. C **37**, 1026 (1988).

[113] A. S. Umar, M. R. Strayer, P.-G. Reinhard, K. T. R. Davies, and S.-J. Lee, Phys. Rev. C **40**, 706 (1989).

[114] C. Bottcher, M. R. Strayer, A. S. Umar, and P.-G. Reinhard, Phys. Rev. A **40**, 4182 (1989).

[115] A. S. Umar and V. E. Oberacker, Phys. Rev. C **73**, 054607

[116] J. A. Maruhn, P.-G. Reinhard, P. D. Stevenson, and A. S. Umar, Comp. Phys. Comm. **185**, 2195 (2014).

[117] E. Chabanat, P. Bonche, P. Haensel, J. Meyer, and R. Schaeffer, Nucl. Phys. A **635**, 231 (1998).

[118] P. A. M. Guichon, H. H. Matevosyan, N. Sandulescu, and A. W. Thomas, Nucl. Phys. A **772**, 1 (2006).

[119] P. Klüepfel, P.-G. Reinhard, T. J. Bürvenich, and J. A. Maruhn, Phys. Rev. C **79**, 034310 (2009).

[120] M. Kortelainen, T. Lesinski, J. More, W. Nazarewicz, J. Sarich, N. Schunck, M. V. Stoitsov, and S. Wild, Phys. Rev. C **82**, 024313 (2010).

[121] A. S. Umar and V. E. Oberacker, Phys. Rev. C **74**, 021601 (2006).

[122] A. S. Umar, V. E. Oberacker, J. A. Maruhn, and P.-G. Reinhard, Phys. Rev. C **80**, 041601 (2009).

[123] A. S. Umar and V. E. Oberacker, Eur. Phys. J. A **39**, 243 (2009).

[124] A. S. Umar and V. E. Oberacker, Phys. Rev. C **74**, 024606 (2006).

[125] A. S. Umar and V. E. Oberacker, Phys. Rev. C **77**, 064605 (2008).

[126] A. S. Umar and V. E. Oberacker, Phys. Rev. C **74**, 061601 (2006).

[127] Ka–Hae Kim, Takaharu Otsuka, and Paul Bonche, J. Phys. G **23**, 1267 (1997).

[128] V. E. Oberacker, A. S. Umar, E. Terán, and A. Blazkiewicz, Phys. Rev. C **68**, 064302 (2003).

[129] A. Blazkiewicz, V. E. Oberacker, A. S. Umar, and M. Stoitsov, Phys. Rev. C **71**, 054321 (2005).

[130] R. Rafiei, R. G. Thomas, D. J. Hinde, M. Dasgupta, C. R. Morton, L. R. Gasques, M. L. Brown, and M. D. Rodriguez, Phys. Rev. C **77**, 024606 (2008).

[131] R. G. Thomas, D. J. Hinde, D. Duniec, F. Zenke, M. Dasgupta, M. L. Brown, M. Evers, L. R. Gasques, M. D. Rodriguez, and A. Diaz-Torres, Phys. Rev. C **77**, 034610 (2008).

[132] C. Yadav, R. G. Thomas, R. K. Choudhury, P. Sugathan, A. Jhingan, S. Appannababu, K. S. Golda, D. Singh, Ish Mukul, J. Gehlot, E. Prasad, and H. J. Wollersheim, Phys. Rev. C **86**, 034606 (2012).

[133] A. Shamlath, M. Shareef, E. Prasad, P. Sugathan, R. G. Thomas, A. Jhingan, S. Appannababu, A. K. Nasirov, A. M. Vinodkumar, K. M. Varier, C. Yadav, B. R. S. Babu, S. Nath, G. Mohanto, Ish Mukul, D. Singh, and S. Kailas, Nucl. Phys. A **945**, 67 (2016).

[134] M. G. Itkis, A. A. Bogachev, I. M. Itkis, J. Kliman, G. N. Knyazheva, N. A. Kondratiev, E. M. Kozulin, L. Krupa, Y. Oganessian, I. V. Pokrovsky, E. V. Prokhorova, and A. Rusanov, Nucl. Phys. A **787**, 150 (2007).

[135] E. V. Prokhorova, A. A. Bogachev, M. G. Itkis, I. M. Itkis, G. N. Knyazheva, N. A. Kondratiev, E. M. Kozulin, L. Krupa, Y. Oganessian, I. V. Pokrovsky, V. V. Pashkevich, and A. Rusanov, Nucl. Phys. A **802**, 45 (2008).

[136] V. E. Viola, K. Kwiatkowski, and M. Walker, Phys. Rev. C **31**, 1550 (1985).

[137] D. J. Hinde, J. R. Leigh, J. J. M. Bokhorst, J. O. Newton, R. L. Walsh, and J. W. Boldeman, Nucl. Phys. A **472**, 318 (1987).